"Fe-F and Al-F avoidance rule" in ferrous-aluminous (OH, F) biotites

"Fe–F and Al–F avoidance rule" in ferrous-aluminous (OH,F) biotites

by *B. Boukili[1], F. Holtz[2], J.-M. Bény[3] and J.-L. Robert[3]*

Abstract

The results of infrared and Raman spectroscopic investigations in the OH-stretching and lattice-mode regions in synthetic ferrous-aluminous (OH,F)-biotites are presented. In the OH-stretching region (3800–3200 cm^{-1}), all micas studied present a high intensity peak at high frequencies [3669 cm^{-1} for (OH)-annite and 3641 cm^{-1} for (OH)-Es] which can be decomposed into two bands and a low intensity peak at low frequencies [3535 cm^{-1} for (OH)-annite and 3589 cm^{-1} for (OH)-Es] which suggests rather a vacant octahedral site. Along the (OH,F)-annite join, the intense peak at 3669 cm^{-1} shifts to lower frequencies as X_F increases from 0 to 0.4. In contrast, this peak shifts to higher frequencies along the (OH,F)-Es join (Es = $K(Fe_{2.25}Al_{0.75})(Si_{2.25}Al_{1.75})O_{10}(OH,F)_2$). The low-intensity V-band remains roughly unchanged.

The two bands that compose the 3669 cm^{-1} peak are assigned to a N-band resulting from OH–$Fe^{2+}Fe^{2+}Fe^{2+}$ (Tri-6$^+$) vibrations and a Ib-band due to OH–$Fe^{2+}Fe^{2+}Al^{3+}$ (Tri-7$^+$) vibrations. As the amount of fluorine increases in micas of the (OH,F)-annite join, the N-band frequency varies weakly but its intensity decreases significantly, while the Ib-band becomes more intense. In contrast, these two bands show an opposite behaviour in (OH,F)-Es micas. The N-band intensity increases whereas that of the Ib-band decreases.

The opposite evolution of the two main bands in the OH-stretching region shows that F is preferentially linked to Fe rather than to Al in (OH,F)-annite, whereas F is preferentially linked to Al rather than to Fe in (OH,F)-Es. Consequently, the bond strengths Al–F or Fe–F are not controlled by the Fe–F or Al–F avoidance rule (which would predict that fluorine is preferentially associated to Fe in all micas), but by structural constraints. The Al–F or Fe–F avoidance rule may not play a determining role on the fluorine content of the micas as it is generally agreed. The maximum fluorine contents in micas mainly depend on the ability of the dimensional adaptation of tetrahedral and octahedral layers.

Keywords: Fluorine, trioctahedral ferrous micas, Fe–F and Al–F avoidance rule, infrared and Raman spectroscopy.

Introduction

Numerous experimental studies have been performed on (OH,F)-biotite coexisting with fluids because the composition of this mineral can provide valuable information on the fluorine content of the coexisting minerals or fluids. These studies involve stability and phase relations of (OH,F)-biotite (MUNOZ and LUDINGTON, 1969, 1974; MUNOZ, 1984), synthesis and characterization of biotites by vibrational spectroscopy (LEVILLAIN, 1982; DYAR and BURNS, 1986; ROBERT et al., 1993; PAPIN et al.,

1997), by NMR (SANZ and STONE, 1979, 1983), and by EXAFS (MANCEAU et al., 1990), and finally crystal-chemical approaches for modelling the OH → F substitution in biotite (MASON, 1992; ROBERT et al., 1993; BOUKILI et al., 1993; EARLEY et al., 1995). The most important conclusions from these studies are that F → OH substitution is mainly governed by (1) the activity of hydrofluoric acid (f_{HF}) in the fluid in equilibrium with biotite, (2) temperature, (3) composition (4) the entropy of the F ↔ OH exchange reaction between biotite and hydrothermal fluid, and (5) crystal-chemical constraints.

[1] Faculté des sciences de Rabat. Département des sciences de la Terre, UFR geoappl, BP 1014, Rabat-Maroc.
  <boukili@fsr.ac.ma>
[2] Universität Hannover, Institut für Mineralogie, Welfengarten 1, D-30167 Hannover.
[3] CNRS-CRSCM, Orléans, 45071-Cedex 02, France.

Indeed, it is clear now that the composition, in particular X_{Mg}, and the related structural features of biotite play an important control on cation distributions and fluorine content of this mineral. Fluorine anions are linked preferentially to Mg rather than to Fe. This phenomenon is known as the Fe–F avoidance rule, which is observed in ferrous-aluminous biotites as well. In such biotites, the fluorine content of annite (iron endmember of biotite), expressed as $X_F = F/(OH + F)$, is slightly higher than in aluminum-annite when these micas are equilibrated with the same fluid phase (MUNOZ and LUDINGTON, 1974). Octahedral aluminum content in Al-annite has little effect on F $\leftrightarrow$ OH exchange because Al–F bonds are less favorable owing of the greater strength of Fe–F (RAMBERG, 1952). As outlined by MUNOZ (1984), the observed differences of log K_{Sid} < log K_{Ann} may be related to this fluorine behaviour.

Biotite-(OH,F) composition and the "Fe–F and/or Al–F avoidance rule" seem to affect significantly the cation distributions in and between octahedral and tetrahedral layers and F/(OH+F) ratio in these micas. The focus of the present work is to analyze the relationship between the composition, cation distributions and fluorine content of ferrous-aluminous biotites by using infrared and Raman spectrometry. These techniques will elucidate the structural constraints on F $\rightarrow$ OH substitution mechanisms. To our knowledge, the effect of F $\rightarrow$ OH substitution on infrared and Raman spectra of annite has never been analyzed. In this study, these two spectroscopic techniques are used to characterize several biotite compositions with various fluorine contents along the annite-siderophyllite join.
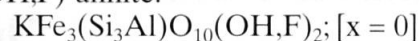
Experimental and analytical Methods

Starting materials were gels prepared according to the method of HAMILTON and HENDERSON (1968). Potassium was introduced as dried K_2CO_3 transformed to nitrate by nitric acid attack, silicon as tetraethyl orthosilicate (TEOS), aluminium and one part of iron (50%) as nitrate. Finally, fluorides (KF, AlF_3 or FeF_2 and metallic iron (Fe^0) were mechanically added to the gels to obtain the appropriate bulk compositions. Based on results of previous works (LEVILLAIN 1979; MONIER and ROBERT, 1986; JULLIOT et al. 1987), it could be shown that the addition of iron as Fe^{3+} (nitrate) and Fe^0 in ratio Fe^{3+}/Fe^0 equal to 1 is the best technique to reach rapidly the Fe^{3+}/Fe^{2+} equilibrium in experimental products synthesized at low oxygen fugacities The compositions of the trioctahedral F-free micas studied are expressed by:
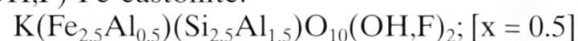
$$K(Fe_{3-x}Al_x)(Si_{3-x}Al_{1+x})O_{10}(OH)_2$$
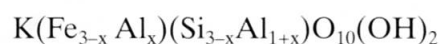
where x corresponds to the amount of Tschermak-type substitution. The F $\rightarrow$ OH substitution has been studied along three (OH,F)-joins:

(OH,F)-annite:
$KFe_3(Si_3Al)O_{10}(OH,F)_2$; [x = 0]
(OH,F)-Fe-eastonite:
$K(Fe_{2.5}Al_{0.5})(Si_{2.5}Al_{1.5})O_{10}(OH,F)_2$; [x = 0.5]
(OH,F)-Es:
$K(Fe_{2.25}Al_{0.75})(Si_{2.25}Al_{1.75})O_{10}(OH,F)_2$; [x = 0.75]

The last join corresponds to a composition intermediate between Fe-eastonite (x = 0.5) and siderophyllite (x = 1).

Syntheses were performed in vertical Tuttle-type pressure vessels with water as the pressure medium. Temperature was measured using Ni–NiCr thermocouples calibrated against the melting points of NaCl and $ZnCl_2$. Temperature uncertainty is less than ±5 °C. Pressures were measured with a Bourdon gauge, with an uncertainty of less than ±5 MPa. All experiments were performed at 720 °C, 100 MPa P_{H2O}, with a duration of 7 days. At this temperature, equilibrium is reached after three days, a length of 7 days has been adopted to improve the cristallinity of micas. Oxygen fugacity was controlled by the double capsule method of EUGSTER (1957), using the magnetite-wüstite (MW) assemblage as a solid buffer introduced with water in the external Au-capsule. More experimental details are given by BOUKILI et al. (2001).

The run products were examined with a petrographic microscope and by scanning electron microscopy (SEM). X-ray diffraction was used to check if the products are composed of a single phase or of a multiple phase assemblage and to characterize the mica. Diffraction patterns were obtained between $5° \leq 2\theta \leq 65°$, the radiation used was Co-Kα (λ = 1.7902 Å). The interplanar distances d_{001} (= c sinβ) and d_{060} (= b/6) were systematically measured using Si as an internal standard. The (OH,F)-micas analyzed in this study are labeled on the basis of the bulk atomic fluorine fraction (X_F = F/OH+F) of the starting gels. This value of X_F does not necessarily correspond to that of the synthesized micas because of the partitioning of fluorine between the fluid phase and minerals and because some run products are composed of additional phases which can also incorporate fluorine. However, in order to check the nominal values of X_F, wet chemical analyzes have been done on 30 to 40 mg of the run products obtained along the (OH,F)-annite join. For run products composed of pure annite, only small de-

viations were observed from the values of X_F in the starting gels (see Table 1 in BOUKILI et al., 2001).

Infrared data were obtained at room temperature with a Nicolet 710 spectrometer. Samples were prepared as KBr pellets, with a mineral to KBr ratio of 5% by weight for investigation in the frequency range (3800–3200 cm^{-1}) and 0.2% by weight for the low-frequency range (1200–400 cm^{-1}). The resolution was 2 cm^{-1}. Raman spectra were recorded on a XY DILOR spectrometer equipped with an argon-ion laser (Innova 90-5, λ_0 = 514.5 nm) operating between 10 and 20 mW at the sample. Integration times ranged from 600 to 2400 s. The detector used is a multichannel (CCD) in conjunction with "Notch" filter which allows us to obtain a high signal/noise. The resolution in peak positions is 2 cm^{-1}. The spectra (IR and Raman) were fitted to the sum of lines with Lorentzian shape using the program Peakfit. Small deviations between raw and fitted spectra were generally observed at high-frequencies side of N-bands; this is due to the CHRISTIANSEN effect (1884).

For the decomposition of the infrared spectra in the OH-stretching vibration range (3800–3200 cm^{-1}), we have adopted the nomenclature of VEDDER (1974) coupled to that proposed by BOUKILI (1995) and REDHAMMER et al. (2000) on ferrous-aluminous biotites: N-bands (also defined as Tri-6$^+$), due to OH groups bonded to three octahedrally coordinated divalent cations (3Fe^{2+}), in which the OH dipole is close to the c* axis; I-bands (Tri-5$^+$ or 6$^+$), due to OH groups bonded to

two divalent (Fe^{2+}) and one trivalent cation (Fe^{3+} or Al^{3+}, respectively Ia and Ib), OH dipole is slightly tilted from the c* axis; V-bands (Di-5$^+$ or 6$^+$), due to OH groups adjacent to one octahedral vacancy and two octahedrally coordinated cations ([Fe^{2+}Al^{3+}]; [Fe^{2+}Fe^{3+}]; [Fe^{3+}Al^{3+}]; [Fe^{3+}Fe^{3+}] labelled Va, Vb, Vb' and Vc, respectively), the OH dipole is approximately within the (001) plane. "Tri" and "Di" refer to trioctahedral and dioctahedral environments around OH dipole, while 6$^+$ or 7$^+$ indicate the bulk number of charges of octahedral cations. Generally, the frequencies of N-type bands are the highest, and those of the V-type bands are the lowest (ROBERT and KODAMA, 1988). The intensity of the bands resulting from dioctahedral environments around OH is much higher than that resulting from trioctahedral environments (ROUXHET, 1970; SANZ et al., 1983, 1984). The intensity is higher for I-type bands than for the N-band (ROUSSEAUX et al., 1972). In the frequency range of the lattice vibrations (1200–350 cm^{-1}), the assignment of the bands is based on the results along the annite-siderophyllite join obtained by BOUKILI (1995) and REDHAMMER et al. (2000).

Experimental products

Detailed discussions of run products and the lattice parameters of these trioctahedral micas are given in BOUKILI et al. (2001). Briefly, the results show that the OH → F substitution is low in all

Table 1 Infrared assignments of ferrous biotites in the frequency range of hydroxyl stretching vibrations.

OH-stretching wavenumbers (cm^{-1})	VEDDER (1964) Natural biotite	WILKINS (1967) Natural biotite	FARMER et al. (1971) Natural biotite	GILKES et al. (1972) Natural biotite	FARMER (1974) Synthetic annite
Assignment					
3530	–	–	–	OH–Fe^{2+}Fe^{3+}☐	–
3541	–	–	OH–Fe^{2+}Fe^{3+}☐	–	OH–Fe^{2+}Fe^{3+}☐
3550	OH–M^{3+}M^{3+}☐	–	–	–	–
3580	–	–	–	–	–
3600	OH–M^{2+}M^{3+}☐	–	OH–Fe^{2+}Al^{3+}☐	–	–
3620	OH–M^{2+}M^{2+}☐	–	–	–	–
3664	–	OH–Fe^{2+}Fe^{2+}Fe^{2+}	–	–	–

|	LEVILLAIN and MAUREL (1980)	RANCOURT et al.(1994) Synthetic annite MW–720°C	BOUKILI (1995) Synthetic annite	REDHAMMER et al. (2000) Synthetic annite	Band–type Synthetic annite
	OH–Fe^{3+}Fe^{3+}☐ or OH–Fe^{2+}Fe^{3+}☐	–	OH–Fe^{3+}Fe^{3+}☐ OH–Fe^{2+}Fe^{3+}☐	OH–Fe^{3+}Fe^{3+}☐ OH–Fe^{2+}Fe^{3+}☐	Vc or Vb
3530–3535					
3540–3545	–	OH–Fe^{2+}Fe^{2+}Fe^{3+}	–	–	–
3575–3580	OH–Fe^{2+}Al^{3+}☐	OH–Fe^{2+}Fe^{2+}Al^{3+}	–	–	–
3624–3628	OH–Fe^{2+}Fe^{2+}Fe^{3+}	–	OH–Fe^{2+}Fe^{2+}Fe^{3+}	OH–Fe^{2+}Fe^{2+}Fe^{3+}	Ia
3650	–	–	OH–Fe^{2+}Fe^{2+}Al^{3+}	OH–Fe^{2+}Fe^{2+}Al^{3+}	Ib
3664–3668	OH–Fe^{2+}Fe^{2+}Fe^{2+}	OH–Fe^{2+}Fe^{2+}Fe^{2+}	OH–Fe^{2+}Fe^{2+}Fe^{2+}	OH–Fe^{2+}Fe^{2+}Fe^{2+}	N
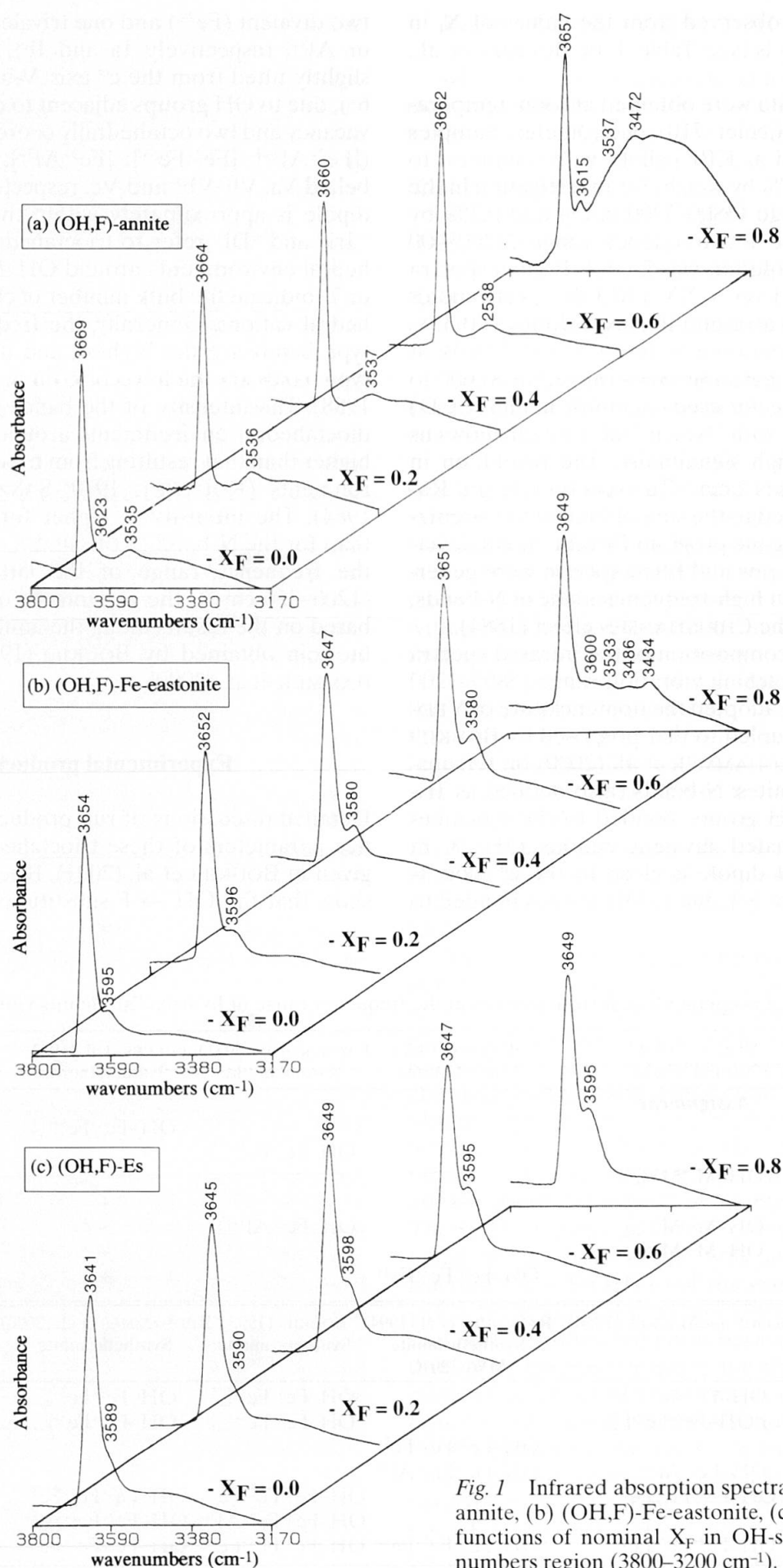
Fig. 1 Infrared absorption spectra of (a) (OH,F)-annite, (b) (OH,F)-Fe-eastonite, (c) (OH,F)-Es as functions of nominal X_F in OH-stretching wavenumbers region (3800–3200 cm^{-1}).

investigated micas (the saturation of fluorine in the mica is attained with the appearance of additional phases, such as quartz, topaz, magnetite and glass). In (OH,F)-annite, fluorine solubility is attained at $X_{ann-F} = 0.5$ (annite is observed as the only phase in products of experiments with $X_F = 0$ to $X_F = 0.5$), and it is more restricted for aluminous compositions (OH,F)-Fe-eastonite and (OH,F)-Es at $X_{Al-ann-F} = 0.2$. For $X_{ann-F} \geq 0.6$, mica coexists with topaz, quartz, and a low refractive-index phase that is probably glass. At $X_{Al-ann-F} > 0.2$, the run product was a mixture of mica, topaz, glass and an unidentified phase. In fact, there is an inverse correlation between octahedral aluminum and fluorine content in the micas that may be due to the Al–F avoidance rule in agreement with the results obtained on metamorphic phlogopites by GUIDOTTI (1984).

Infrared and Raman data in the OH-stretching and lattice vibrations range

(OH,F)-ANNITE

Infrared spectra obtained from micas with various fluorine contents are shown in Fig. 1. The intense peak at 3669 cm^{-1} in the OH-annite end-member shifts to lower frequencies with increasing X_F in the range $0 \leq X_F \leq 0.4$ (Fig. 2). For compositions with higher fluorine contents the frequency changes slowly but the mole fraction of fluorine in biotite becomes a nonlinear function of X_F for these compositions. Thus, this change cannot be attributed to the fluorine content of biotite because of the presence of topaz in the run products. At low frequencies, two bands are recognized in the range 3630–3530 cm^{-1} (Fig. 1a). The first one, at 3623 cm^{-1}, is not well resolved. The low intensity of this band results in part from the low [6]Fe^{3+} contents present in these samples, as has been shown by Mössbauer study (less than 3% of the total Fe is as [6]Fe^{3+}; BOUKILI et al., 2001). This band desappears with increasing Al content toward Fe-eastonite and (OH)-Es. Therefore, this band which is sensitive to both the Al content and Fe^{2+}/Fe^{3+} ratio must be assigned to an Ia-type (Tri-7$^+$, OH–$Fe^{2+}Fe^{2+}Fe^{3+}$; Table 1) in agreement with the previous studies of (LEVILLAIN and MAUREL, 1980, Table 1). This Ia-band desappears also progressively as fluorine increases till $X_F = 0.4$–0.6 and becomes again more pronouced at high X_F (Fig. 1a). The second band, observed at 3535 cm^{-1} for $X_F = 0$, is classically assigned to a Vb and/or Vc-bands of type Di-5$^+$ or Di-6$^+$ respectively, due to OH groups adjacent to octahedral vacancies and bonded to $Fe^{3+}Fe^{2+}$ or $Fe^{3+}Fe^{3+}$ (GILKES et al.,

1971; FARMER, 1974; LEVILLAIN and MAUREL, 1980; REDHAMMER et al., 2000, Table 1). This band remains unchanged as fluorine increases and is the only Fe^{3+}-bearing octahedral environment.

Decompositions of the infrared and Raman spectra in OH-stretching range are shown in Figs. 3a and 4a. The intense peak resulting from the OH-stretching vibrations clearly shows contributions of two bands. The band at ≈ 3668 cm^{-1} is assigned to stretching mode of OH groups in the vicinity of three octahedrally coordinated Fe^{2+} (WILKINS, 1967; FARMER, 1974; LEVILLAIN and MAUREL, 1980). It is therefore an N-band of type Tri-6$^+$. The decompositions of spectra (Figs. 3 and 4) shows also that the intensity of N-band decreases and that of the band at 3650 cm^{-1} (OH-annite) increases as the (OH)-annite becomes more Al-rich composition. This band was assigned to OH–$Fe^{2+}Fe^{2+}Al^{3+}$, an Ib-type band Tri-7$^+$ by BOUKILI (1995) and REDHAMMER et al. (2000). As fluorine contents increase, the intensity of the low frequency Ib-band increases at the expense of that of the high frequency (Figs. 3 and 4). In Raman spectra, we note that the Ia-band and the V-band have not been resolved owing to their weak intensity.

In the region of the lattice vibrations, the frequencies of most bands vary as fluorine contents increase in the system (Fig. 5a). Two intense broad bands are observed around 986 and 457 cm^{-1} in the F-free annite. They are assigned respectively to Si–O$_{\parallel}$ stretching vibrations [transition moment roughly parallel ($\parallel$) to the cleavage plane (001)] and to bending vibrations Si–O–Si com-
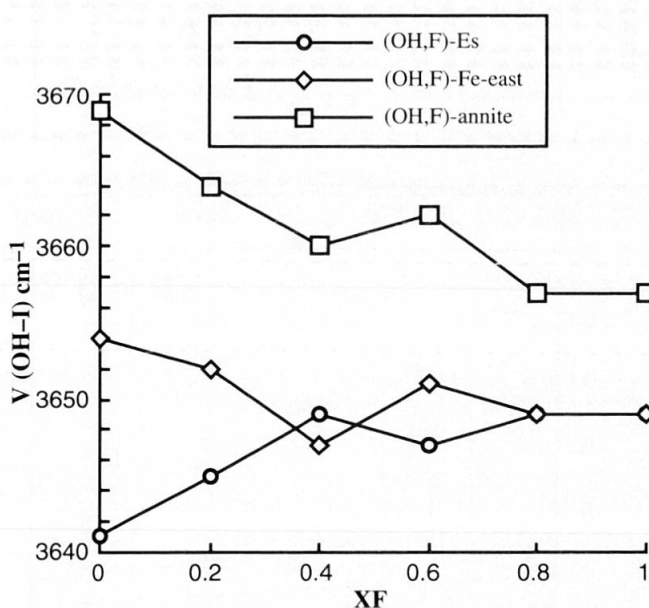

Fig. 2 Evolution of ν_{OH} (intense peak, N + Ib-bands) stretching wavenumbers in cm^{-1} of the micas studied as a function of nominal X_F.

(a) (OH,F)-annite

$X_F = 0.0$

$-Fe^{2+}Fe^{2+}Fe^{2+}$

$-Fe^{2+}Fe^{2+}Al3^+$

$-Fe^{2+}Fe^{2+}Fe3^+$

$-Fe^{2+}Fe3^+\square$

$X_F = 0.2$

(b) (OH,F)-Fe-eastonite

$X_F = 0.0$

$-Fe^{2+}Fe^{2+}Fe^{2+}$

$-Fe^{2+}Fe^{2+}Al3^+$

$-Fe^{2+}Al3^+\square$

$-Fe^{2+}Fe3^+\square$

$X_F = 0.2$

(c) (OH,F)-Es

$X_F = 0.0$

$-Fe^{2+}Fe^{2+}Fe^{2+}$

$-Fe^{2+}Fe^{2+}Al3^+$

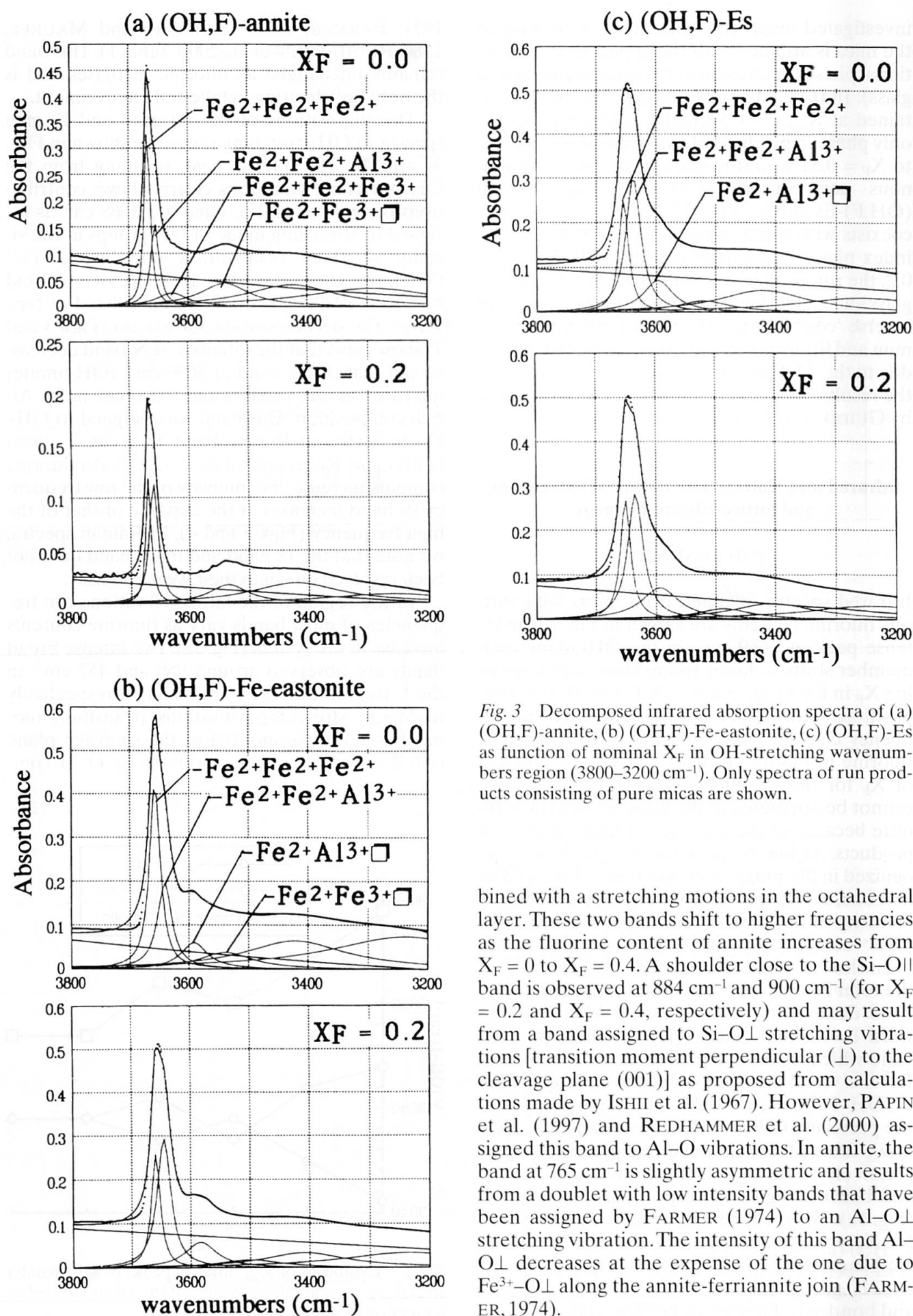$-Fe^{2+}Al3^+\square$

$X_F = 0.2$

Fig. 3 Decomposed infrared absorption spectra of (a) (OH,F)-annite, (b) (OH,F)-Fe-eastonite, (c) (OH,F)-Es as function of nominal X_F in OH-stretching wavenumbers region (3800–3200 cm⁻¹). Only spectra of run products consisting of pure micas are shown.

bined with a stretching motions in the octahedral layer. These two bands shift to higher frequencies as the fluorine content of annite increases from $X_F = 0$ to $X_F = 0.4$. A shoulder close to the Si–O∥ band is observed at 884 cm⁻¹ and 900 cm⁻¹ (for $X_F = 0.2$ and $X_F = 0.4$, respectively) and may result from a band assigned to Si–O⊥ stretching vibrations [transition moment perpendicular (⊥) to the cleavage plane (001)] as proposed from calculations made by ISHII et al. (1967). However, PAPIN et al. (1997) and REDHAMMER et al. (2000) assigned this band to Al–O vibrations. In annite, the band at 765 cm⁻¹ is slightly asymmetric and results from a doublet with low intensity bands that have been assigned by FARMER (1974) to an Al–O⊥ stretching vibration. The intensity of this band Al–O⊥ decreases at the expense of the one due to Fe^{3+}–O⊥ along the annite-ferriannite join (FARMER, 1974).

(a) (OH,F)-annite

$X_F = 0$

Fe2+Fe2+Fe2+

Fe2+Fe2+Al3+

$X_F = 0.2$

wavenumbers (cm-1)

(b) (OH,F)-Fe-eastonite

$X_F = 0$

Fe2+Fe2+Fe2+

Fe2+Fe2+Al3+

$X_F = 0.2$

wavenumbers (cm-1)

(c) (OH,F)-Es

$X_F = 0$

Fe2+Fe2+Fe2+

Fe2+Fe2+Al3+

Fe2+Al3+☐
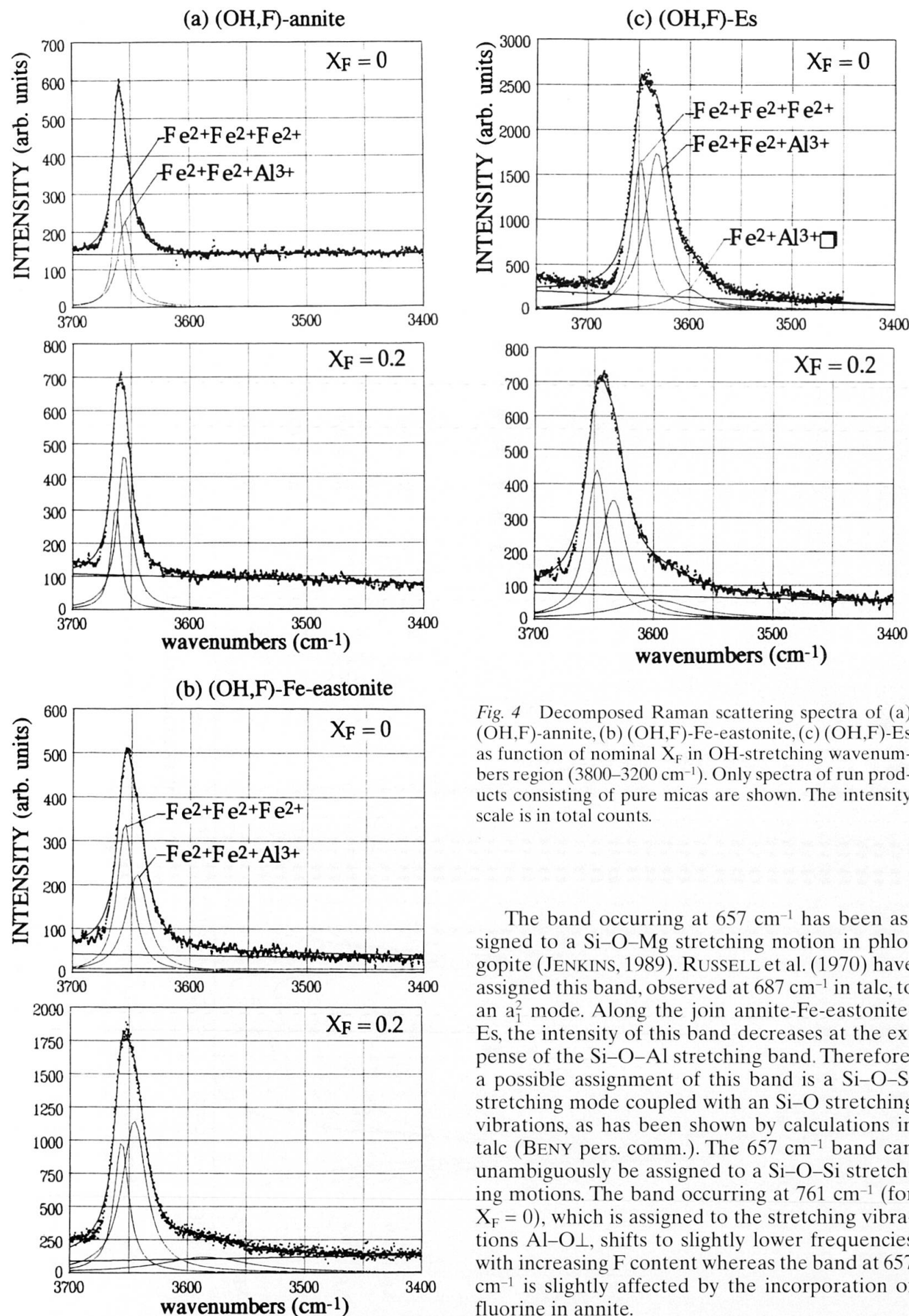
$X_F = 0.2$

wavenumbers (cm-1)

Fig. 4 Decomposed Raman scattering spectra of (a) (OH,F)-annite, (b) (OH,F)-Fe-eastonite, (c) (OH,F)-Es as function of nominal X_F in OH-stretching wavenumbers region (3800–3200 cm-1). Only spectra of run products consisting of pure micas are shown. The intensity scale is in total counts.

The band occurring at 657 cm-1 has been assigned to a Si–O–Mg stretching motion in phlogopite (JENKINS, 1989). RUSSELL et al. (1970) have assigned this band, observed at 687 cm-1 in talc, to an a_1^2 mode. Along the join annite-Fe-eastonite-Es, the intensity of this band decreases at the expense of the Si–O–Al stretching band. Therefore, a possible assignment of this band is a Si–O–Si stretching mode coupled with an Si–O stretching vibrations, as has been shown by calculations in talc (BENY pers. comm.). The 657 cm-1 band can unambiguously be assigned to a Si–O–Si stretching motions. The band occurring at 761 cm-1 (for $X_F = 0$), which is assigned to the stretching vibrations Al–O⊥, shifts to slightly lower frequencies with increasing F content whereas the band at 657 cm-1 is slightly affected by the incorporation of fluorine in annite.
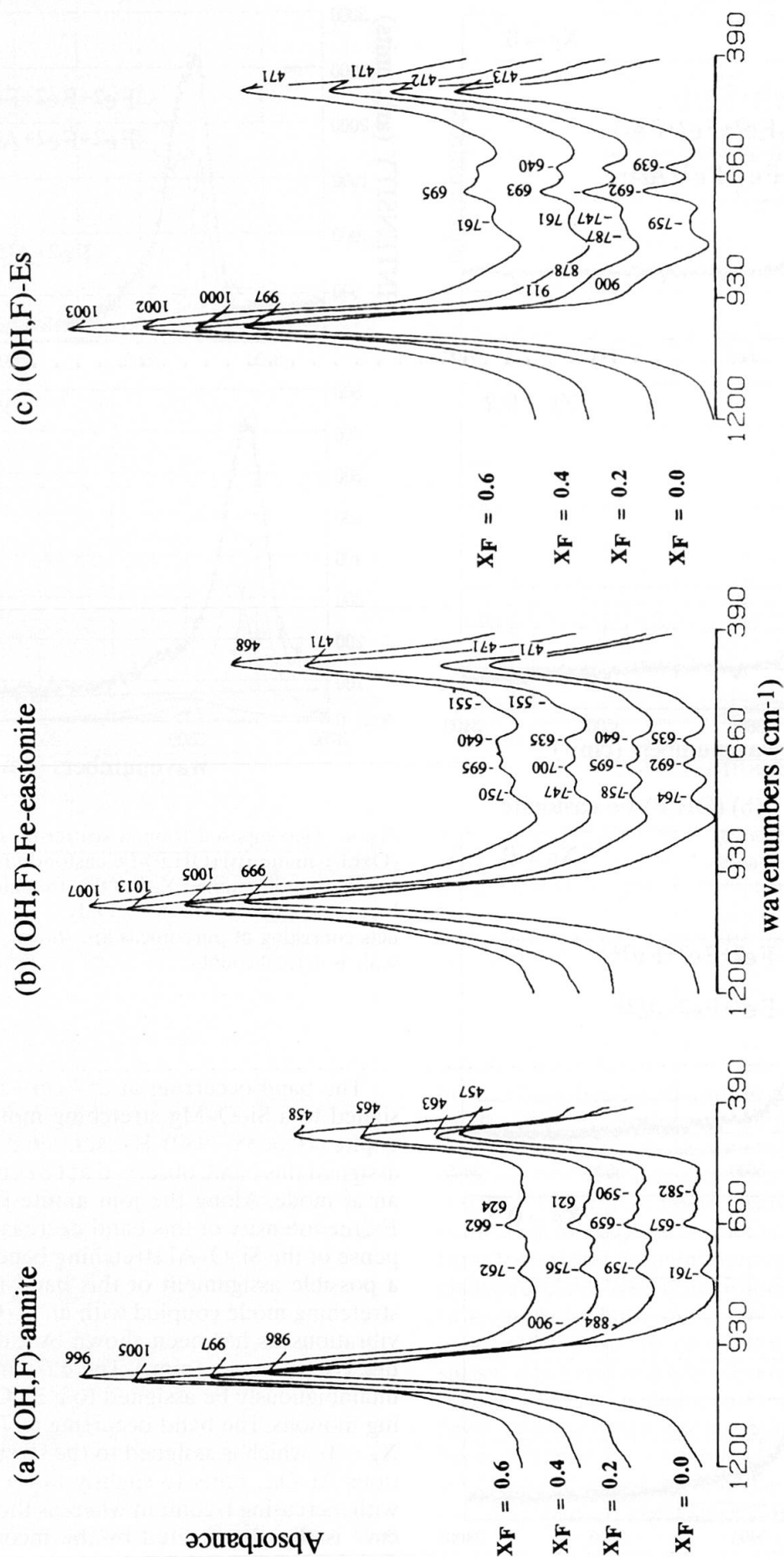
Fig. 5   Infrared absorption spectra of (a) (OH,F)-annite, (b) (OH,F)-Fe-eastonite, (c) (OH,F)-Es as function of nominal X_F in lattice vibrations region (1400–400 cm^{-1}).

Finally, the intensity of bands at 582 cm^{-1}, which is assigned by FARMER (1974) to OH-libration vibrations, clearly decreases when fluorine is incorporated in the structure of annite.

(OH,F)-FE-EASTONITE

In the OH-Fe-eastonite end-member (Fig. 1b), the main (intense and wide) band that occurs at 3654 cm^{-1} shifts to lower frequencies for $X_F \leq 0.4$ (Fig. 2). The shoulder observed at 3595 cm^{-1} remains unchanged in products consisting of a single mica phase ($0 \leq X_F \leq 0.2$). This shoulder is assigned to the vibrations of OH adjacent to a vacancy and Fe^{3+}, Al^{3+} octahedrally coordinated cations (Vb'-band, Di-6$^+$). With increasing fluorine contents, this band at 3595 cm^{-1} becomes progressively better resolved and splits into several dioctahedral components at $X_F = 0.8$. However, some of these bands may be related to the presence of the additional phases (for example, the band at 3434 cm^{-1} is probably from topaz).

The decompositions of the infrared and Raman spectra in the OH-stretching range are shown in Figs. 3b and 4b. The behaviour of OH-Fe-estonite with increasing F-content is similar to that observed for (OH,F)-annite.

In the region of the lattice vibrations, although only two compositions are completely devoid of additional phases ($X_F = 0$ and $X_F = 0.2$), the bands at 999 cm^{-1} (Si–O||), at 692 cm^{-1} and at 635 cm^{-1} (Si–O–Al) shift to higher frequencies with increasing X_F from 0 to 0.2. The general effect of the substitution F $\rightarrow$ OH in micas on the spectra is similar to that observed in (OH,F)-annite (Fig. 5b).

(OH,F)-ES

The effects induced by the F $\rightarrow$ OH substitution in annite and Fe-eastonite differ from those observed for the compositions (OH)-Es (Fig. 1c). Compared to (OH,F)-annite, the frequency of the intense band at 3641 cm^{-1} increases with F content (Fig. 2), for products consisting of pure micas with $0 \leq X_F \leq 0.2$. In contrast, the Vb'-band occurring at 3589 cm^{-1} does not shift significantly for micas with $X_F \leq 0.2$. Beyond $X_F \geq 0.4$ this band (assigned to assigned OH–$Fe^{3+}Al^{3+}\square$ vibrations) becomes more intense and better resolved. The evolution of the infrared and Raman OH-bands intensities is different from that observed for (OH,F)-Fe-eastonite and annite (Figs. 3c and 4c). As the fluorine content increases in (OH,F)-Es (from $X_F = 0$ to 0.2), the intensity of the high frequency band (N-type) increases at the expense of the low frequency band (Ib-type).

In the region of lattice vibrations, it is noteworthy that the effects induced by the OH $\rightarrow$ F substitution on the spectra are similar to those observed in (OH,F)-annite and (OH,F)-Fe-eastonite (Fig. 5c). However, the Si–O$\perp$ band at 900 cm^{-1} is wider than in (OH,F)-annite, and the peak related to Al–O$\perp$ vibrations (around 759 cm^{-1} for $X_F = 0$) clearly results from the contribution of two bands. This phenomenon is interpreted to result from a decrease in the number of OH dipoles in the mica structure, since the F $\rightarrow$ OH substitution eliminates the interactions between OH and the neighbouring tetrahedral oxygens and/or cations in octahedral sites as has been shown by Mössbauer study (BOUKILI et al., 2001).

Discussion

One of the most interesting results is the contrasting effect of the substitution F $\rightarrow$ OH on the evolution of infrared bands in (OH,F)-annite by comparison to (OH,F)-Es. The decomposition of infrared and Raman spectra shows that the main peak in the frequency range 3700–3600 cm^{-1} results from the contribution of two bands (N-type or OH–$Fe^{2+}Fe^{2+}Fe^{2+}$ and Ib-type or OH–$Fe^{2+}Fe^{2+}Al^{3+}$). The evolution of the intensity of these bands with changing F content in annite is the opposite of that observed in Es.

In annite-(OH,F), fluorine preferentially occupies OH-sites with $Fe^{2+}Fe^{2+}Fe^{2+}$ as nearest neighbours (as result of the intensity increase of Ia-type band). This behaviour is in agreement with the thermodynamic model of RAMBERG (1952) which predicts that the association F–Fe is favoured compared to the association F–Al. The variations of the ν_{OH} as a function of X_F are often considered to result either from the compensation of charge imbalances on apical oxygens of tetrahedra by the remaining hydroxyl dipoles (ROBERT et al., 1993) or from the coulombic attraction between the alkalis and fluorine (ROBERT et al., 1999). Both processes can explain the decrease of ν_{OH} (intense peak: N-type + Ib-type, Fig. 1) in annite with increasing F content. However, the increase of that ν_{OH} with increasing F content in (OH,F)-Es remains to be explained.

For Es, the effect of fluorine on the evolution of ν_{OH} (N+Ib-band) is opposite to that observed in (OH,F)-annite: fluorine preferentially occupies OH-sites with $Fe^{2+}Fe^{2+}Al^{3+}$ as nearest neighbours. This inverse behaviour suggests that neither of the processes cited above can explain the evolution of ν_{OH} and that the results of RAMBERG (1952) and ROSENBERG and FOIT (1977) cannot be applied systematically to explain the differ-

ence in equilibrium constants between annite and siderophyllite as proposed by MUNOZ (1984). In conclusion, we note that the OH–$Fe^{2+}Fe^{2+}Fe^{2+}$ site is the only one which is occupied in annite, whereas fluorine preferentially occupies OH-sites adjacent to $Fe^{2+}Fe^{2+}Al^{3+}$.

These spectroscopic observations have structural implications. The dimensional changes due to the increase of Fe^{3+} in the octahedral layer at the expense of the tetrahedral layer along the (OH,F)-annite join are not the result of structural changes in the octahedral layer due to the substitution $[Fe^{2+}O_4(OH)_2] \leftrightarrow [Fe^{2+}O_4(F)_2]$, as suggested by RANCOURT et al. (1996). The dimensional changes most probably result from a preferential substitution of F by OH in $Fe^{2+}Fe^{2+}Fe^{2+}$ environments in case of (OH,F)-annite and in $Fe^{2+}Fe^{2+}Al^{3+}$ environments in case of (OH,F)-Es. This is probably the result of different distortions of the octahedral sites, depending on the presence of Fe or Al.

It is worth noting that the intensity decrease of the Ia band at 3623 cm^{-1}, which is assigned to OH–$Fe^{2+}Fe^{2+}Fe^{3+}$ (Tri-7$^+$), with increasing F content of annite allows clarification of the effect of fluorine on the Fe^{3+} sites in micas, a question which has already been formulated by MASON (1992). F–Fe^{3+} bonds, as well as bonds between F and Li^+, Mn^{2+}, and Ti^{4+}, questioned by MASON (1992), seem not to be governed by avoidance rules but rather by the structural constraints of the mica.

In the low-wavenumbers region of annite spectra, the intensity of the Vc-band remains relatively unchanged for the (OH,F)-annite join (0 ≤ X_F ≤ 0.5). The existence of this band confirms the ferric doublet observed in Mössbauer spectra (BOUKILI et al., 2001). In the aluminous micas (OH,F)-Fe-eastonite and (OH,F)-Es the intensity of Vb'-band increases, and a splitting of these bands is observed for higher X_F values. This behaviour is expected because it has been shown that the substitution of OH adjacent to vacancies with F is difficult (ROBERT et al., 1993).

In the range of lattice vibrations, the frequency of the band assigned to stretching Si–O|| vibrations increases with increasing X_F in all compositions. This effect suggests that the Si–O bond length decreases with the substitution of OH for F as a result of a higher distortion of the tetrahedra. This distortion can be related to the absence of interactions between OH and the basal bridging oxygens (OH···O_b) in F-bearing environments. Such interactions are favoured in Al-rich micas to compensate the charge deficiency resulting from the $[4]Si \rightarrow [4]Al$. In summary, our results, combined with those of RUTHERFORD (1973), EARLEY et al. (1995), RANCOURT et al. (1996), BOUKILI et

al. (2001), show that the substitution F → OH in annite, as well as the Tschermak substitution in this mica, produce a decrease in the b cell parameter, in Fe^{3+} contents, in the Mössbauer quadrupole splitting, in ν_{OH} (intense peak) and an increase in the isomeric shift, in $\nu_{Si-O//}$, ν_{K-O} (mode III) and in the tetrahedral rotation angle (α).

Concluding remarks

– F → OH substitution influences the distribution of cations in octahedral layers, but the avoidance rule Al–F and Fe–F cannot be verified systematically for all biotite compositions. The fluorine content of biotite is controlled by structural factors and not directly by the Al–F and Fe–F bond strength.

– Fe^{2+}–F, Al^{3+}–F, as well as bonds between Fe^{3+} and F are not governed by avoidance rules but rather by structural constraints of the mica.

– The dimensional misfits between octahedral and tetrahedral layers are not the result of the structural changes in the octahedral layer due to the substitution $[Fe^{2+}O_4(OH)_2] \leftrightarrow [Fe^{2+}O_4(F)_2]$. The dimensional changes most probably result from a preferential substitution of F by OH in $Fe^{2+}Fe^{2+}Fe^{2+}$ environments in case of (OH,F)-annite and in $Fe^{2+}Fe^{2+}Al^{3+}$ environments in case of (OH,F)-Es.

– Fluorine is preferentially associated with trioctahedral environments as compared to dioctahedral environments, which explains the higher flourine contents in biotite compared to coexisting muscovite (e.g, in peraluminous two mica granites).

References

BOUKILI, B. (1995): Cristallochimie des biotites ferro-alumineuses dans le système: Na_2O-K_2O-FeO-Fe_2O_3-Al_2O_3-SiO_2-H_2O-HF. Analyse par spectrométries vibrationnelles et Mössbauer. Thèse, Univ. Orléans France, 320 pp.

BOUKILI, B., ROBERT, J.-L. and LAPERCHE, V. (1993): Solid solution range and crystal chemical characterization of trioctahedral micas in the system: K_2O-FeO-Fe_2O_3-Al_2O_3-SiO_2-H_2O-HF, at 600 °C, 1 kbar. Terra Abstracts. 5, 485.

BOUKILI, B., ROBERT, J.-L., BENY., J-M. and HOLTZ, F. (2001): Structural effects of OH → F substitution in trioctahedral micas of the system: K_2O-FeO-Fe_2O_3-Al_2O_3-SiO_2-H_2O-HF. Schweiz. Mineral. Petrogr. Mitt. 81, 55–67.

CHRISTIANSEN, C. (1884): Untersuchungen über die optischen Eigenschaften von fein verteilten Körpern. Wiedemann Ann. Phys. 23, 298–306.

DYAR, M.D. and BURNS, R.G. (1986): Mössbauer spectral study of ferruginous one-layer trioctahedral micas. Am. Mineral. 71, 951–961.

EARLEY III, D., DYAR, M.D., ILTON, E.S. and GRANTHEM, A.A. (1995): The influence of structural fluorine on biotite oxidation in copper-bearing aqueous solutions at low temperatures and pressures. Geochim. Cosmochim. Acta 59, 2423–2433.

EUGSTER, H.P. (1957): Stability of annite. Carnegie Institution of Washington Yearbook, 1956–57, 161–164.

FARMER, V.C. (1974): The layer silicates. In: FARMER, V.C. (ed.): The infrared spectra of minerals. Mineral. Soc. London Monogr. 4, 331–363.

FARMER, V.C, RUSSELL, J.D. and McHARDY, W.J. (1971): Evidence for loss of protons and octahedral iron from oxidized biotites and vermiculites. Mineral. Mag. 38, 122–137.

GILKES, R.J., YOUNG, R.C. and QUIRK, J.P. (1972): The oxidation of octahedral iron in biotite. Clays and Clay Minerals 20, 303–315.

GUIDOTTI, C.V. (1984): Micas in metamorphic rocks. Rev. Mineral. 13, 357–467.

HAMILTON, D.L. and HENDERSON, C.B.M. (1968): The preparation of silicate compositions by a gelling method. Mineral. Mag. 36, 632–838.

ISHII, M., SHIMANOUCHI, T. and NAKAHIRA, M. (1967): Far infrared absorption spectra of layer silicates. Inorg. Chim. Acta 1, 387–392.

JENKINS, D.M. (1989): Empirical study of the infrared lattice vibrations (1100–350 cm^{-1}) of phlogopite. Phys. Chem. Minerals 16, 408–414.

JUILLOT, J.-Y., VOLFINGER, M. and ROBERT, J.-L. (1987): Experimental study of carboirite and related phases in the system: GeO_2-SiO_2-Al_2O_3-FeO-H_2O at pressure up to 2 kbar. Mineral. Petrol. 36, 51–69.

LEVILLAIN, C. (1979): Contribution de la spectrométrie Mössbauer et infrarouge à la caractérisation cristallochimique des micas lithiques et des sidérophyllites. Thèse de 3ème cycle, Univ. Paris VII, 158 pp.

LEVILLAIN, C. and MAUREL, P. (1980): Etude par spectrométrie infrarouge des fréquences d'élongation du groupement hydroxyl dans des micas synthétiques de la série annite-phlogopite et annite-sidérophyllite. C. R. Acad. Sci., Paris, 290, 1289–1292.

LEVILLAIN, C. (1982): Influence des substitutions cationiques et anioniques majeures sur les spectres Mössbauer et Infrarouge des micas potassiques trioctaédriques. Applications cristallochimiques. Thèse d'Etat, Univ. Paris VI, 158 pp.

MANCEAU, A., BONNIN, D., STONE, W.E.E. and SANZ, J. (1990): Distribution of Fe in octahedral sheet of trioctahedral micas by polarised EXAFS. Comparison with NMR results. Phys. Chem. Minerals 17, 363–370.

MASON, R.A. (1992): Models of order and iron-fluorine avoidance in biotite. Can.Mineral. 30, 343–354.

MONIER, G. and ROBERT, J.-L.(1986): Muscovite solid solution in the system: K_2O-MgO-FeO-Al_2O_3-SiO_2-H_2O: An experimental study at 2 kbar PH_2O and comparaison with natural Li-free white micas. Mineral. Mag. 50, 257–266.

MUNOZ, J.L. (1984): F–OH and Cl–OH exchange in micas with applications to hydrothermal deposits. Rev. Mineral. 13, 469–493.

MUNOZ, J.L. (1969): Experimental control of fluorine reactions in hydrothermal systems. Am. Mineral. 54, 943–959.

MUNOZ, J.L. and LUDINGTON, S.D. (1974): Fluoride-hydroxyl exchange in biotite. Am. J. Sci. 274, 396–413.

PAPIN, A., SERGENT, J. and ROBERT, J.-L. (1997): Intersite OH-F distribution in an Al-rich phlogopite. Eur. J. Mineral. 9, 501–508.

RAMBERG, H. (1952): Chemical bonds and the distribution of cations in silicates. J. Geol. 60, 331–335.

RANCOURT, D.G., CHRISTIE, I.A.D., ROYER, M., KOMADA, H., ROBERT, J.-L, LALONDE, A.E. and MURAD, E. (1994): Accurate $^{[4]}Fe^{3+}$ $^{[6]}Fe^{3+}$ and $^{[6]}Fe^{2+}$ site populations in synthetic annite by Mössbauer spectroscopy. Am. Mineral. 79, 51–62.

RANCOURT, D.G., PING, J.Y., BOUKILI, B. and ROBERT, J.-L. (1996): Octahedral-site Fe^{2+} quadripole splitting distribution from Mössbauer spectroscopy along the (OH,F)-annite join. Phys. Chem. Minerals 23, 63–71.

REDHAMMER, G.J., BERAN, A., SCHNEIDER, J., AMTHAUER, G. and LOTTERMOSER, W. (2000): Spectroscopic and structural properties of synthetic micas on the annite-siderophyllite binary: Synthesis, crystal structure refinement, Mössbauer, and infrared spectroscopy. Am. Mineral. 85, 449–465.

ROBERT, J.-L. and KODAMA, H. (1988): Generalization of the correlations between hydroxyl-stretching wavenumbers and composition of micas in the system K_2O-MgO-Al_2O_3-SiO_2-H_2O: A single model for trioctahedral and dioctahedral micas. Am. J. Sci. 288-A, 196–212.

ROBERT, J.-L., BENY, J.-M., DELLA VENTURA, G. and HARDY, M. (1993): Fluorine in micas: crystal-chemical control of the OH-F distribution between trioctahedral and dioctahedral sites. Eur. J. Mineral. 5, 7–18.

ROBERT, J.-L., DELLA VENTURA, G. and HAWTHORNE, F.C. (1999): Near-infrared study of short-range disorder of OH and F in monoclinic amphiboles. Am. Mineral. 84, 68–91.

ROSENBERG, P.E. and FOIT, F.F., JR. (1977): Fe^{2+}–F avoidance in silicates. Geochim. Cosmochim. Acta 41, 345–346.

ROUSSEAUX, J.M., GOMEZ LAVERDE, Y., NATHAN, Y. and ROUXHET, P.G. (1972): Correlation between the hydroxyl stretching bands and the chemical compositions of the trioctahedral micas. Int. Clay Conf. Madrid, Preprint, 1, 117–126.

ROUXHET, P.G. (1970): Hydroxyl stretching bands in micas: A quantitative interpretation. Clay Minerals 8, 375–388.

RUSSELL, J.D., FARMER, V.C. and VELDE, B. (1970): Replacement of OH by OD in layer silicates, and identification of the vibrations of these groups in infrared spectra. Mineral. Mag. 37, 869–879.

RUTHERFORD, M.J. (1973): The phase relations of aluminous iron biotites in the system: $KAlSi_3O_8$-$KAlSiO_4$-Al_2O_3-Fe-O-H. J. Petrol. 14, part 1, 159–80.

SANZ, J. and STONE, W.E.E. (1979): NMR study of micas II. Distribution of Fe^{2+}, F^- and OH^- in the octahedral sheet of phlogopite. Am. Mineral. 64, 119–126.

SANZ, J. and STONE, W.E.E. (1983): NMR applied to minerals: VI. Local order in the octahedral sheet of micas: Fe–F avoidance. Clay Minerals 18, 187–192.

SANZ, J., DE LA CALLE, C. and STONE, W.E.E. (1984): NMR applied to minerals. V. The localization of vacancies in the octahedral sheet of aluminous biotites. Phys. Chem. Minerals 11, 235–240.

VEDDER, W. (1964): Correlation between infrared spectrum and chemical composition of micas. Am. Mineral. 49, 736–768.

WILKINS, R.W.T. (1967): The hydroxyl-stretching region of biotite mica spectrum. Mineral. Mag. 36, 325–333.